ISSN 0036-0244, Russian Journal of Physical Chemistry A, 2023, Vol. 97, No. 9, pp. 2044–2051. © Pleiades Publishing, Ltd., 2023.

ELECTROCHEMISTRY. GENERATION AND STORAGE OF ENERGY FROM RENEWABLE SOURCES

Research on Corrosion Inhibitors for Coatings on Hot-Dip Aluminized-Galvanized Steel in Marine Environment

Zhenkai Xu[a], Lian Chen[a], Jingliang Han[a], and Chengfei Zhu[a,*]

[a]*College of Materials Science and Engineering, Nanjing Tech University, Nanjing, Jiangsu, 211800 China*

** e-mail: Njtechzhucf@163.com*

Received November 20, 2022; revised December 17, 2022; accepted December 19, 2022

Abstract—Galvanized steel is one of the commonly used material in the field of corrosion protection, but it's prone to corrosion in heavily corrosive environments. Hence, the Hot-Dip Aluminized-Galvanized Steel (HDAGS) was developed, which is less susceptible to corrosion, by adding aluminum to the galvanizing solution. But in marine environment, the HDAGS still requires further protection. In this article, the effect of nine common corrosion inhibitors on HDAGS was evaluated by Immersion corrosion test, Tafel polarization, EIS test, XRD, SEM&EDS firstly. The results showed that the adsorbed film inhibitors and the deposited film inhibitors were effective, but the oxidized film inhibitors were not ideal because the Al–Zn coating was hard to oxidize. The corrosion rate of HDAGS in simulated seawater containing 1 wt % zinc phosphate was 3.333×10^{-7} g/(m^2 h), while it was 6.072×10^{-4} g/(m^2 h) in simulated seawater without inhibitor, and the inhibition efficiency was 99.94%. Three most effective inhibitors were then added to the waterborne polyurethane coating (WPUC) for HDAGS, and the performance was evaluated by EIS and Immersion corrosion test. The impedance of WPUC containing inhibitors all decreased fast at the beginning of immersion. The subsequent action of the corrosion inhibitor in the corrosion process extended the service life of WPUC by 2–3 times.

Keywords: corrosion inhibitor, hot-dip aluminized-galvanized steel (HDAGS), marine environment, waterborne polyurethane (WPUC)

DOI: 10.1134/S0036024423090285

1. INTRODUCTION

The hot-dip aluminized-galvanized steel (HDAGS) (55%Al–43.4%Zn–1.6%Si, wt %) was a highly corrosion-resistant coated steel developed by Bethlehem Steel in the United States. It was widely used in marine construction, equipment and other fields because of its corrosion and oxidation resistance [1–3]. However, several elements, such as Cl and S, could destabilize it, resulting in the acceleration of corrosion, which limited its application and development [4–6]. Therefore, further protective technologies were required. The corrosion inhibitors were more applicable because it had the advantages of simple operation, less dosage and high efficiency compared with other methods [7, 8].

The research on corrosion inhibitors for HDAGS hadn't been carried out for now, but the researchers had made certain progress on aluminum and zinc alloys corrosion inhibitors. Ma et al. [9] studied the effect of L-cysteine/ZnO compound inhibitor on the corrosion resistance of aluminum alloy in alkaline environment. The results showed that the compound inhibitor significantly reduced the anode corrosion rate by controlling the diffusion process of Zn^{2+}. Zhao et al. [10] studied the inhibition effect of phthalocyanine sulfonate on 7075 aluminum alloy in acidic environment. Phthalocyanine was verified as a hybrid corrosion inhibitor because it was validated to adsorb to aluminum by molecular dynamics simulations and XPS analysis. Anyiam et al. [11] extruded galvanized steel by starch physically and evaluated its corrosion inhibition effect in 1 M HCl. It was found that the modified starch belonged to a hybrid corrosion inhibitor by electrochemical method, and its adsorption process obeyed the Langmuir adsorption isotherm. Meeusen et al. [12] applied odd random phase electrochemical impedance spectroscopy (ORP-EIS) to study the time-effect. Silica-based and phosphate-based corrosion inhibitors were evaluated for hot-dip galvanized steel in 0.05 M NaCl.

In order to fill the research gap of HDAGS's corrosion inhibitors, the effect of nine common corrosion inhibitors for HDAGS was evaluated in simulated marine environment by Immersion corrosion test, Tafel polarization, EIS test, XRD, SEM&EDS in this paper. Effective corrosion inhibitors were added to the WPUC to assess their influence on the comprehensive performance of coatings.

2. EXPERIMENTAL

2.1. Synthesis

HDAGS (Baoshan Iron and Steel Co.) was cut into rectangular coupons, whose size were 50 × 25 × 1 mm^3. The HDAGS coupons were immersed in ammonium acetate (CH_3COONH_4) solution with the concentration of 10 wt % at 70°C for 5 min first to remove the oxide and then cleaned in deionized water. 5 wt % medium alkaline degreasing agent was applied to degrease the HDAGS coupons' surface by ultrasonic cleaning for 5 min. After washing with deionized water, the HDAGS coupons were soaked in absolute ethanol, then dried with cold air for use. The simulated seawater was configured according to the Mocledon formula [13]. The specific components of the simulated seawater were as follows: sodium chloride 26.726 g/L, magnesium chloride 2.26 g/L, magnesium sulfate 3.248 g/L, calcium chloride 1.153 g/L, sodium bicarbonate 0.198 g/L, potassium chloride 0.721 g/L, sodium bromide 0.058 g/L, boric acid 0.058 g/L, sodium silicate 0.0024 g/L, disodium tetrasilicate 0.0015 g/L, phosphoric acid 0.002 g/L, aluminium chloride 0.013 g/L, ammonia 0.002 g/L, lithium nitrate 0.0013 g/L. Corrosion inhibitors were added to the simulated seawater by 1 wt %. The corrosion inhibitors were as followed: disodium L-(+)-tartrate, sodium molybdate, gluconic acid, sodium salt, *N*-methyldiethanolamine, benzimidazole, triethanolamine, calcium carbonate, 2-mercaptobenzimidazole, and zinc phosphate. The medicines used were purchased from Shanghai Aladdin Co. The specific groups of simulated seawater containing corrosion inhibitors are shown in Table 1.

The selected inhibitors were added to the WPUC at a ratio of 1 wt %. Magnetic stirred at 25°C for 6 h. The WPUC with and without inhibitor were roll-coated on HDAGS coupons with an RDS wire rod coater (#3, USA) [14], then dried at 200°C for 37 s. The immersion time of the coated HDAGS coupons in the simulated seawater was extended to 400 h to obtain a complete corrosion process.

Table 1. Groups of simulated seawater containing different inhibitors

Group	Corrosion inhibitor
A	Blank (simulated seawater without inhibitor)
B	Disodium L-(+)-tartrate
C	Sodium molybdate
D	Gluconic acid, sodium salt
E	*N*-Methyldiethanolamine
F	Benzimidazole
G	Triethanolamine
H	Calcium carbonate
I	2-Mercaptobenzimidazole
J	Zinc phosphate

2.2. Characterization

The microstructure and composition of HDAGS coupons were observed by a scanning electron microscope (SEM, HITACHI S-4800, Japan) equipped with an energy dispersive spectrometer (EDS) [15]. The composition of the corrosion product was determined by an X-ray diffractometer (XRD, Rigaku, Japan) [16]. The scanning speed was 10 deg/min in the 2θ ranges from 10° to 90°.

The effect of corrosion inhibitors on the HDAGS coupons and WPUC were evaluated by static immersion test. The corrosion area of HDAGS was obtained referring to ISO4628. The corrosion rate of HDAGS after being immersed was calculated by formula (1). The inhibition efficiency was calculated by formulas (2) and (3)

$$V\pm = \frac{m_0 - m_1}{St}, \quad (1)$$

$$\eta = \frac{V_0 - V_1}{V_0}, \quad (2)$$

$$\eta = \frac{Jcorr_0 - Jcorr_1}{Jcorr_0}, \quad (3)$$

where $V\pm$ was the corrosion rate, g/(m^2 h); m_0 was the HDAGS coupons' mass before corrosion, g; m_1 was the HDAGS coupons' mass after corrosion, g; S was the area exposed to the solution, m^2; t was corrosion time, h; η was the inhibition efficiency, %; V_0 and V_1 were the corrosion rates of HDAGS coupons in the simulated seawater without and with corrosion inhibitor, g/(m^2 h), respectively; $Jcorr_0$ and $Jcorr_1$ were the self-corrosive current density of HDAGS coupons in the simulated seawater without and with corrosion inhibitor, A/cm^2, respectively.

Potentiodynamic polarization curves and AC Impedance spectroscopy (EIS) tests of HDAGS coupons with and without WPUC coated were performed in simulated seawater at 25°C via Solartron 1260 + 1287 electrochemical workstation. The saturated Hg/Hg_2Cl_2 electrode and graphite electrode were used as the reference electrode and counter electrode [17], respectively. During the potentiodynamic polarization measurements, the potential was swept from −300 to +300 mV (vs. open circuit potential) using a scan rate of 1 mV/s. The EIS data were obtained in the frequency range of ~10^5–10^{-3} Hz with an amplitude of 5 mV at open circuit potential.

3. RESULTS AND DISCUSSION

3.1. Static Immersion Test

Table 2 was the corrosion rate of HDAGS in different groups, which was calculated by static immersion corrosion test. The corrosion rate of HDAGS in simulated seawater without inhibitor (Group A) was 6.072×10^{-4} g/(m^2 h), and the thickness index was 1.151×10^{-3} mm/yr. Disodium L-(+)-tartrate (Group B) would accelerate the corrosion of HDAGS, while other inhibitors played a certain degree of corrosion inhibition effect on HDAGS in simulated seawater, among which the best inhibitor was zinc phosphate (Group J). The corrosion rate was 3.333×10^{-7} g/(m^2 h), the thickness index was 6.319×10^{-7} mm/yr, and the inhibition efficiency was up to 99.94%.

Table 2. Corrosion rate of HDAGS in simulated seawater of different groups

Group	Corrosion rate, g m^{-2} h^{-1}	Thickness index, mm yr^{-1}	Inhibition efficiency, %
A	6.072×10^{-4}	1.151×10^{-3}	—
B	8.930×10^{-4}	1.693×10^{-3}	–47.07
C	3.893×10^{-4}	7.380×10^{-4}	35.89
D	3.738×10^{-4}	7.086×10^{-4}	38.44
E	9.680×10^{-5}	1.835×10^{-4}	84.19
F	2.314×10^{-5}	4.386×10^{-5}	96.19
G	1.664×10^{-5}	3.154×10^{-5}	97.26
H	9.008×10^{-7}	1.708×10^{-6}	99.85
I	7.041×10^{-7}	1.335×10^{-6}	99.88
J	3.333×10^{-7}	6.319×10^{-7}	99.94

3.2. Electrochemical Test

Figure 1 showed the potentiodynamic polarization curves of HDAGS coupons in simulated seawater containing different inhibitors at 25°C. Figure 2 presented the electrochemical impedance spectroscopy of HDAGS coupons in simulated seawater of different groups. Figures 3a, 3b were the equivalent circuit model of HDAGS in simulated seawater without and with different inhibitors, where Rs was the solution resistance, CPE was the constant phase angle element, Rf was the resistance of HDAGS, CPEdl, and Rct were the CPE of the double electric layer and the charge transfer resistance, respectively. Table 3 was the fitted data of the potentiodynamic polarization curves and electrochemical impedance spectroscopy.

It can be seen that the regular of the corrosion current density and impedance values of HDAGS was consistent with static immersion corrosion rate. The effect of deposited film inhibitors (Groups J and H), adsorbed film inhibitors (Groups I, G, F, and E) and oxidized film inhibitors (Groups D, C, and B) were from superior to inferior for HDAGS. Among adsorbed film inhibitors, O atoms of N-methyldiethanolamine and triethanolamine (Groups E and G) were adsorbed, while N atoms of benzimidazole and 2-mercaptobenzimidazole were adsorbed. It can be differentiated from static immersion test and electro-

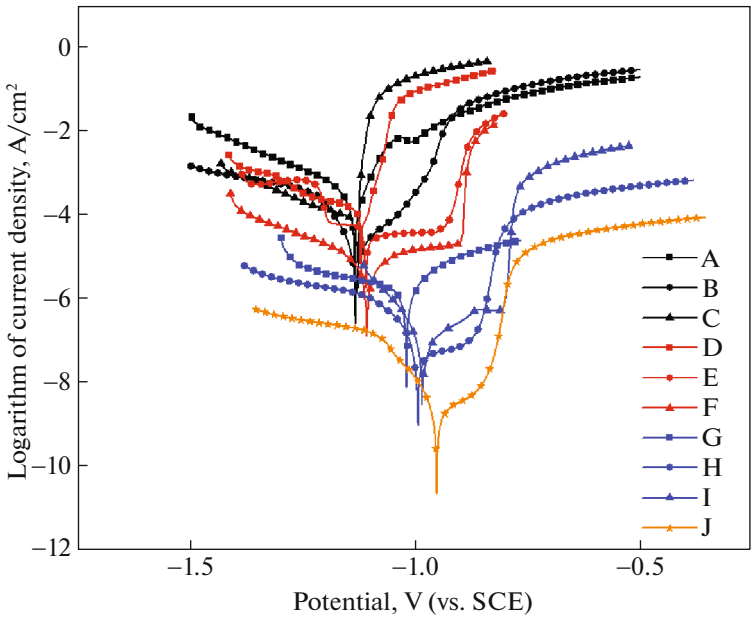

Fig. 1. Polarization curves of HDAGS coupons of different groups in simulated seawater.

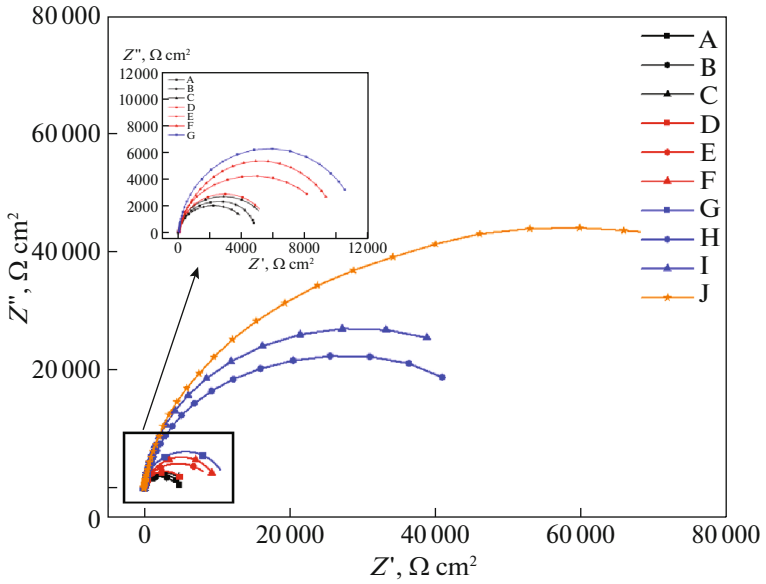

Fig. 2. EIS curves of HDAGS coupons of different groups in simulated seawater.

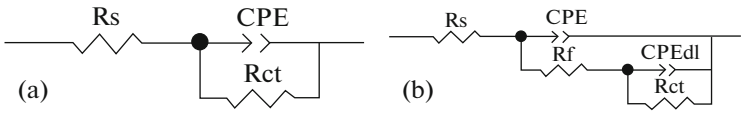

Fig. 3. The equivalent circuit of HDAGS for fitting Nyquist plot.

chemical test that N adsorption (Groups F and I) was better than O adsorption (Groups E and G) for HDAGS. The best corrosion inhibitors were still calcium carbonate, 2-mercaptobenzimidazole, and zinc phosphate. Zinc phosphate and calcium carbonate were deposited film inhibitors [18, 19]. Zn^{2+} and Ca^{2+} could react with CO_3^{2-}, PO_4^{3-}, and OH^- in the cathode region of HDAGS and adhere to the coupons' surface. 2-Mercaptobenzimidazole was an adsorbed film inhibitor [20, 21]. N atoms contained in its benzo heteroring could coordinate with metal ions and firmly adsorbed on HDAGS, thereby isolating the contact between the HDAGS and the corrosive medium.

Table 3. Fitted data of the electrochemical test shown in Figs. 1 and 2

Group	*Jcorr*, A cm^{-2}	Inhibition efficiency, %	Rct, Ω cm^2
A	4.111×10^{-4}	—	5537.07
B	5.572×10^{-4}	–35.52	4804.20
C	2.588×10^{-4}	37.05	5745.12
D	2.328×10^{-4}	43.38	5941.32
E	5.200×10^{-5}	87.35	9045.54
F	1.770×10^{-5}	95.69	11 132.22
G	1.262×10^{-5}	96.93	11844.96
H	6.471×10^{-7}	99.84	56532.00
I	5.309×10^{-7}	99.87	60383.40
J	1.309×10^{-7}	99.97	112636.44

3.3. Characterization of HDAGS after Immersed for 144 h

Figure 4 and Table 4 were SEM morphologies and EDS element composition of HDAGS after immersed in simulated seawater (Groups A, H, I, and J) for 144 h. The deposition film formed by calcium carbonate and zinc phosphate on the surface of HDAGS were

Table 4. EDS analysis of HDAGS after immersed for 144 h

Group	Zn	Al	Fe	Ca	N	P
A	55.88	18.21	1.6	0	0	0
H	7.61	0.38	0.45	60.87	0	0
I	16.92	11.20	1.99	0	1.58	0
J	40.38	1.36	1.51	0	0	8.53

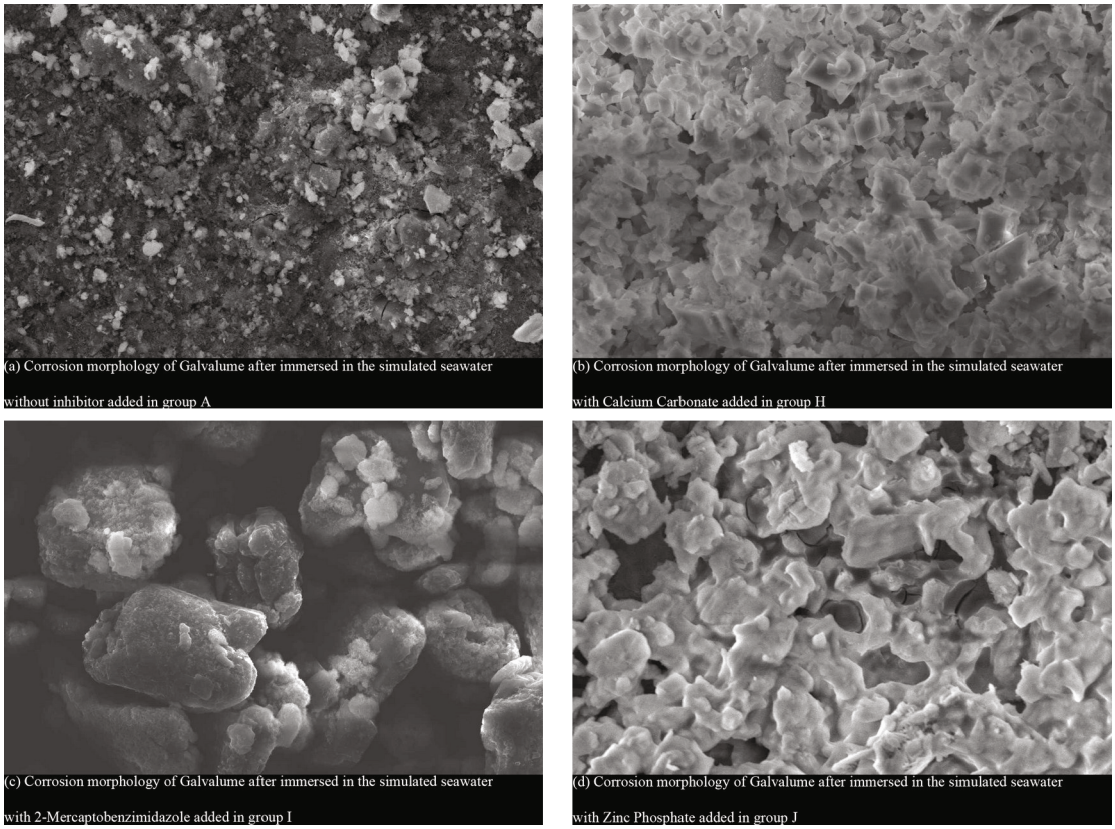

Fig. 4. SEM morphologies of HDAGS after immersed for 144 h.

small and entangled, while 2-mercaptobenzimidazole formed large adsorption film on the surface of HDAGS. The Zn^{2+} and Al^{3+} on the surface of HDAGS promoted the forming a deposition film containing Ca with a content of 60.87 wt %. The higher content of Zn in Group J was due to the formation of the deposition film. 2-Mercaptobenzimidazole was adsorbed film inhibitor, and the adsorption film had less binding force than the deposition film. However, 1.58 wt % N element could also prove the presence of the adsorption film.

The HDAGS was analyzed by XRD in Fig. 5, which were immersed in simulated seawater of Groups A, H, I, and J, respectively. There was no peaks other than the matrix peaks of Al, Zn, and Fe in the XRD pattern of the HDAGS immersed in the simulated seawater without corrosion inhibitors. After doping different inhibitors in simulated seawater, the peaks of matrix presented varying degrees of attenuation, and the element peaks of corrosion inhibitors also began to appear. In the simulated seawater doped with calcium carbonate (Group H), the peak of Al decreased significantly, indicating that part of the coated Al element was consumed during the deposition process, and the peak of $CaCO_3$ (PDF 86-2341) appeared, accompanied by heterogeneous peaks. In the simulated seawater doped with 2-mercaptobenzimidazole (Group I), the peak of $Fe_{16}N_2$ (PDF 78-1865) presented. Element N indicated the occurrence of the adsorption process. In the simulated seawater doped with zinc phosphate (Group J), the peak of $AlPO_4$ (PDF 89-4201) showed up, which indicated the deposition process. Overall, the results of XRD were consistent with SEM&EDS.

3.4. Performance of Composite WPUC

Figure 6 was the corrosion area of WPUC with and without different inhibitors in simulated seawater. The corrosion area of the WPUC with inhibitors expanded much more slowly than the WPUC without inhibitors. The corrosion spot of WPUC without inhibitors was firstly discovered at 96 h, while that of WPUC with inhibitors showed up at 144 h. The rust class of WPUC without inhibitors was Ri5 according to ISO4628, while that of WPUC containing 1 wt % zinc phosphate was Ri4. It proved that the inhibitors could delay corrosion whether it was added to the corrosive medium directly or into the coating. Calculated from the corrosion area, with the addition of corrosion inhibitor, the service life of the WPUC can be extended by 2–3 times.

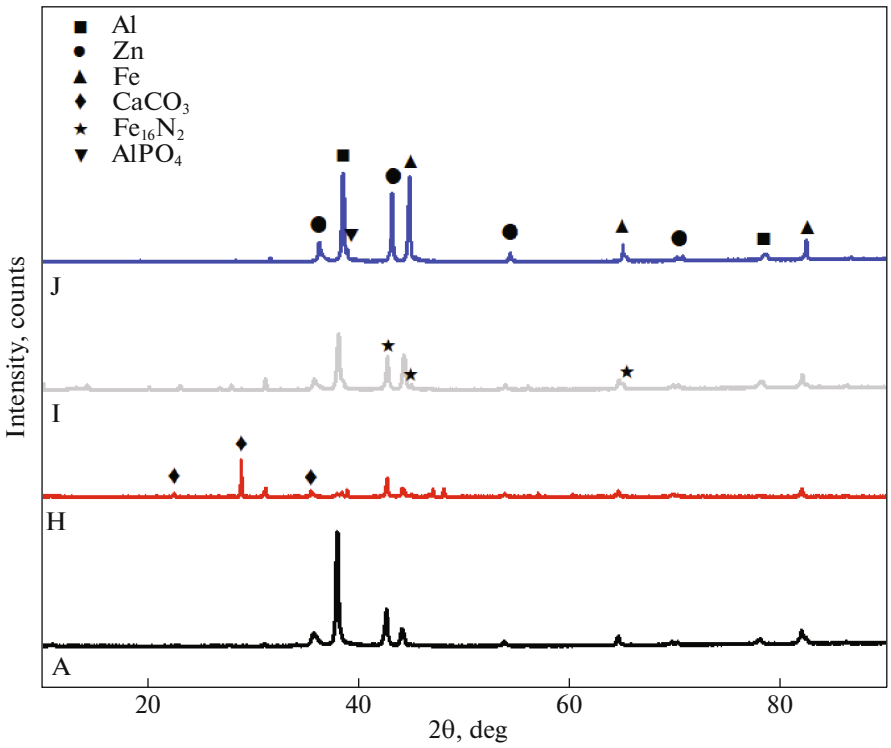

Fig. 5. XRD of HDAGS after immersed in simulated seawater for 144 h (Groups A, H, I, and J).

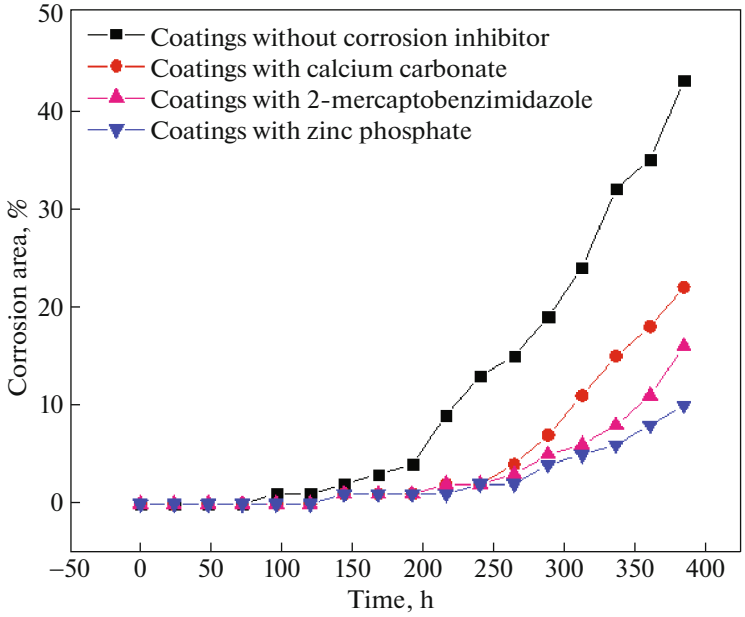

Fig. 6. Corrosion area of WPUC with and without inhibitors in simulated seawater.

Figure 7 presented the curves of the impedance changes of the WPUC with and without inhibitors in simulated seawater at 25°C. After immersed for 12 h, the impedance of all coatings dropped rapidly, which was caused by the dissolution of the coatings in seawater solution [22]. The impedance of WPUC doped with inhibitors were slightly lower than that of WPUC without inhibitors, because the addition of inhibitors

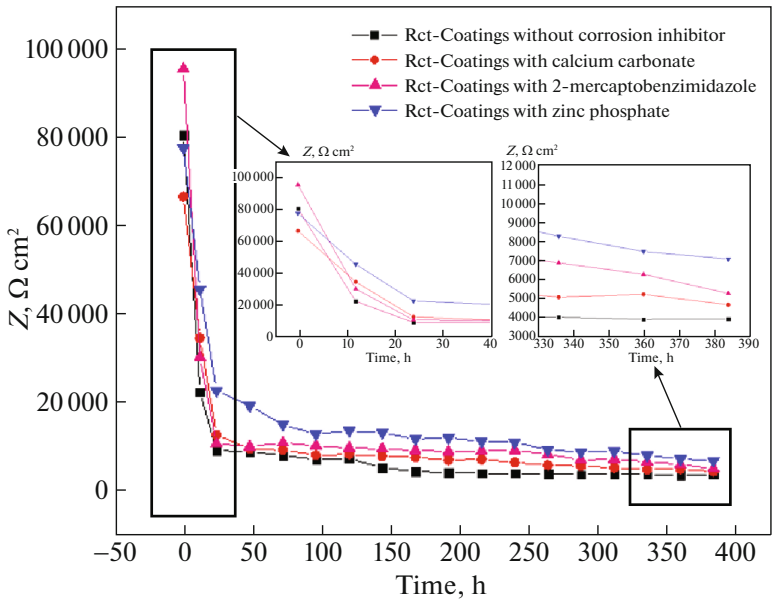

Fig. 7. Impedance changes of WPUC with and without inhibitors in simulated seawater.

changed the resin structure in the coating, resulting in a certain amount of defects. During the immersion process of simulated seawater, the inhibitors formed inhibition film, which worked in tandem with WPUC. In the subsequent immersion test, the impedance of WPUC containing the corrosion inhibitors were always higher than that of WPUC without inhibitors. The impedance of WPUC containing the corrosion inhibitors were consistent with the efficiency of the inhibitors itself.

4. CONCLUSIONS

The influence of nine common corrosion inhibitors on the corrosion behavior of HDAGS in the marine environment was studied in this paper. It was found that the oxidized film inhibitors (Groups B, C, and D) had a poor inhibition effect because the Al–Zn coating was difficult to passivate. The effect of adsorbed film inhibitors varied according to the adsorption element. N adsorption (Groups F and I) was better than O adsorption (Groups E and G). The deposited film inhibitors were the most effective, among which the corrosion current density of HDAGS in simulated seawater containing 1 wt % zinc phosphate was 1.309×10^{-7} A/cm^2, while the corrosion rate of HDAGS in simulated seawater was 4.111×10^{-4} A/cm^2, and the inhibition efficiency was 99.94%. The performance of WPUC containing inhibitors were evaluated, and the impedance all decreased rapidly at the beginning of immersion. The deposited film inhibitors presented to be the most effective, and the service life of WPUC was extended by 2–3 times.

ACKNOWLEDGMENTS

This study was supported by the National Natural Science Foundation of China (grant no. 21203095), the Jiangsu National Synergetic Innovation Center for Advanced Materials (SICAM) and the Priority Academic Program Development of Jiangsu Higher Education Institutions (PAPD).

CONFLICT OF INTEREST

The authors declare that they have no conflicts of interest.

REFERENCES

1. X. Zhang, I. O. Wallinder, and C. Leygraf, Surf. Eng. **34**, 641 (2018).
2. K. A. Yasakau, S. Kallip, A. Lisenkov, et al., Electrochim. Acta **211**, 126 (2016).
3. K. M. Moon, S. Y. Lee, J. H. Jeong, et al., Key Eng. Mater. **744**, 217 (2017).
4. S. Yan, Q. H. Liang, and L. Y. Wen, Int. J. Heat Technol. **40**, 685 (2022).
5. Z. L. Ding, J. Zhang, S. M. Jiang, et al., J. Phys.: Conf. Ser. **2101**, 012078 (2021).
6. T. Prosek, A. Nazarov, F. Goodwin, et al., Surf. Coat. Technol. **306**, 439 (2016).
7. A. Goyal, E. Ganjian, H. S. Pouya, et al., Constr. Build. Mater. **303**, 124461 (2021).
8. M. Y. Karelina, S. M. Gaidar, H. D. Quang, et al., Russ. Eng. Res. **42**, 172 (2022).
9. J. L. Ma, W. H. Li, G. X. Wang, et al., J. Electrochem. Soc. **165**, 266 (2018).
10. P. Zhao, X. L. Han, W. J. Wang, et al., J. Adhes. Sci. Technol. **34** (12), 133 (2020).

11. C. K. Anyiam, O. Ogbobe, E. E. Oguzie, et al., SN Appl. Sci. **2**, 520 (2020).
12. M. Meeusun, L. Zardet, A. M. Homborg, et al., Corros. Sci. **173**, 108780 (2020).
13. H. T. Yue, C. Ling, T. Yang, et al., Biotechnol. Biofuels **7**, 108 (2014).
14. M. Y. Zhang, Y. Wang, H. L. Jiang, et al., J. Phys.: Conf. Ser. **2044**, 012055 (2021).
15. H. Fakhry, M. E. Faydy, F. Benhiba, et al., Colloids Surf., A **610**, 125746 (2021).
16. S. Y. Khazhiev, M. A. Khusainov, R. A. Khalikov, et al., Russ. J. Org. Chem. **56**, 1 (2020).
17. Y. W. Li, J. Zhou, J. Song, et al., Biosens. Bioelectron. **144**, 111534 (2019).
18. J. H. Yue, G. Lou, G. R. Zhou, et al., Mater. Sci. Forum **993**, 1110 (2020).
19. C. V. Nikolopoulos, Eur. J. Appl. Math. **30**, 529 (2019).
20. M. R. Jakeria, R. J. Toh, X. B. Chen, et al., J. Appl. Electrochem. **52**, 1021 (2022).
21. X. C. Wu, F. Wiame, V. Maurice, et al., Appl. Surf. Sci. **527**, 146814 (2020).
22. C. R. Wang, J. H. Wang, S. G. Wen, et al., Corros. Rev. **39**, 339 (2021).